# Absence of $Ni^{2+}/Ni^{3+}$ charge disproportionation and possible roles of O 2$p$ holes in $La_3Ni_2O_{7-\delta}$ revealed by hard x-ray photoemission spectroscopy

D. Takegami [1,2] K. Fujinuma [1] R. Nakamura [1] M. Yoshimura [3] K.-D. Tsuei [3] G. Wang [4,5] N. N. Wang [4,5] J.-G. Cheng [4,5] Y. Uwatoko [6] and T. Mizokawa [1]

[1] *Department of Applied Physics, Waseda University, 3-4-1 Okubo, Shinjuku-ku, Tokyo 169-8555, Japan*
[2] *Max Planck Institute for Chemical Physics of Solids, Nöthnitzer Strasse 40, 01187 Dresden, Germany*
[3] *National Synchrotron Radiation Research Center, 101 Hsin-Ann Road, 30076 Hsinchu, Taiwan*
[4] *Beijing National Laboratory for Condensed Matter Physics and Institute of Physics, Chinese Academy of Sciences, Beijing 100190, China*
[5] *School of Physical Sciences, University of Chinese Academy of Sciences, Beijing 100190, China*
[6] *Institute for Solid State Physics, 5-1-5 Kashiwanoha, Kashiwa 277-8581 Chiba, Japan*

(Received 28 November 2023; revised 12 January 2024; accepted 16 February 2024; published 11 March 2024)

We have investigated the electronic structure of $La_3Ni_2O_{7-\delta}$ ($\delta \approx 0.07$) by means of hard x-ray photoemission spectroscopy (HAXPES). Although the nominal Ni valence is close to +2.5, the Ni 2$p$ HAXPES spectra show an absence of $Ni^{2+}/Ni^{3+}$ charge disproportionation. The Ni 2$p$ spectral shape including the main peak and the charge-transfer satellite indicate that oxygen 2$p$ holes are heavily involved in the transport properties. The spectral weight suppression at the Fermi level indicates that the carriers of O 2$p$ character (mixed with Ni 3$d$) are affected by electronic correlation which would be associated with the density wave transition and the superconductivity controlled by pressure.

DOI: 10.1103/PhysRevB.109.125119

## I. INTRODUCTION

Perovskite-type transition-metal oxides exhibit rich physical properties due to the interplay between spin, charge, and orbital degrees of freedom of transition-metal $d$ electrons [1–3]. Among them, perovskite Ni oxides harbor metal-insulator transitions and exotic superconductivities which are deeply associated with its charge and orbital degrees of freedom. $R$NiO$_3$ ($R$ = rare earth) with a formal Ni valence of +3 exhibits a metal-insulator transition as a function of the ionic radius of the $R$ ion [4]. The insulating phase of $R$NiO$_3$ is accompanied by Ni charge disproportionation between $+(3-\delta)$ and $+(3+\delta)$ with $0 < \delta < 1$ [5]. $BiNiO_3$ exhibits a pressure-induced insulator-to-metal transition with a Ni valence change from +2 to +3 which is associated with its negative thermal expansion behavior [6]. More recently, infinite-layer $R$NiO$_2$ systems with a formal Ni valence close to +1 have been found to show superconductivity upon hole doping [7,8] and their transition temperature can be enhanced under pressure [9]. The rich physical properties of the perovskite-type Ni oxides are derived from their charge and orbital degrees of freedom. The $x^2-y^2$ type Ni 3$d$ $e_g$ orbital is partially occupied and forms an anisotropic Fermi surface in the infinite-layer $R$NiO$_2$. $R$NiO$_3$ and $BiNiO_3$ avoid the Jahn-Teller active low-spin $Ni^{3+}$ by Ni charge disproportionation and by Bi-Ni intermetallic charge transfer, respectively. In addition, the O-to-Ni charge-transfer energy tends to be small in $Ni^{3+}$ oxides [10,11], and oxygen 2$p$ orbitals can be involved in the Ni charge disproportionation [12–14] and by the Bi-Ni intermetallic charge transfer [15].

The recent discovery of pressure-induced high-$T_c$ superconductivity in bilayer perovskite $La_3Ni_2O_{7-\delta}$ [16–18] has fueled interest in perovskite-type Ni oxides. The crystal structure of $La_3Ni_2O_7$ is illustrated in Fig. 1(a). The Ni ion is octahedrally coordinated by six oxygens, and the Ni 3$d$ orbitals are split into $e_g$ ($x^2-y^2$ and $3z^2-r^2$) and $t_{2g}$ ($xy$, $yz$, and $zx$) orbitals. Immediately after the discovery, effective two-band models with Ni 3$d$ $x^2-y^2$ and $3z^2-r^2$ orbitals have been developed to understand the high-$T_c$ superconductivity in bilayer Ni perovskite [19–26]. Liu *et al.* have reported $Ni^{2+}/Ni^{3+}$ charge disproportionation in $La_3Ni_2O_{7-\delta}$ based on the presence of a two-peak structure found in the Ni 2$p$ core level x-ray photoemission spectrum, and assigning them to $Ni^{2+}$ and $Ni^{3+}$ contributions [27]. However, it is known that the electronic configuration of $Ni^{3+}$ is close to $d^8L$ ($L$: oxygen 2$p$ hole) rather than $d^7$ and that the Ni 2$p$ binding energy difference between $Ni^{2+}$ and $Ni^{3+}$ is negligibly small [28–31]. If the electronic configuration of $Ni^{3+}$ is $d^8L$, the situation of $La_3Ni_2O_{7-\delta}$ would be similar to the hole-doped cuprate superconductors with $d^9L$. The superconducting phases of $R$NiO$_2$ and $La_3Ni_2O_{7-\delta}$ may correspond to electron- and hole-doped $d^8$ Mott insulators as illustrated in Fig. 1(b). In this context, it is highly important to reexamine the electronic structure of $La_3Ni_2O_{7-\delta}$ by means of photoemission spectroscopy and clarify whether its ground state should be understood in terms of $d^7-d^8$ configurations or a hole-doped $d^8L-d^8$.

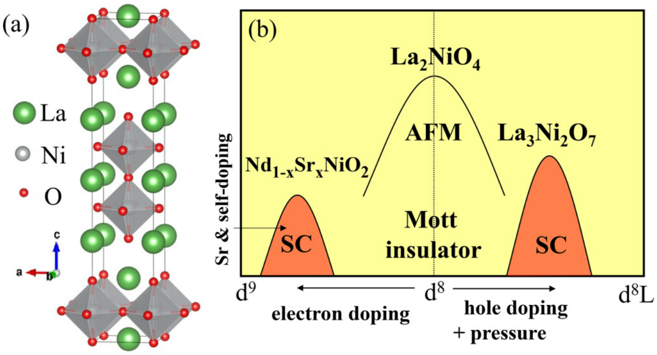


FIG. 1. (a) Crystal structures of an idealized bilayer perovskite, represented using the program VESTA [33]. (b) Schematic suggested phase diagram of nickelates based on electron doping from $d^8$ to $d^9$ and hole doping from $d^8$ to $d^8L$. The electron concentration per Ni of $Nd_{1-x}Sr_xNiO_2$ is reduced from $d^9$ due to Sr doping and partial charge transfer (self-doping) from Ni to Nd [7–9].

In the present paper, in order to solve the puzzle related to the Ni valence and O $2p$ holes and to clarify the fundamental electronic structure of $La_3Ni_2O_{7-\delta}$, we have performed hard x-ray photoemission spectroscopy (HAXPES).

## II. METHODS

Polycrystalline samples of $La_3Ni_2O_{7-\delta}$ ($\delta \approx 0.07$) were prepared via the sol-gel method as reported in the literature [18]. Further details regarding the characterization and the properties of the samples used in the measurements are also found in Ref. [18]. HAXPES measurements were performed at the Max-Planck-NSRRC HAXPES end station with an MB Scientific A-1 HE analyzer, Taiwan undulator beamline BL12XU of SPring-8 [32]. The photon energy was set to 6.5 keV, resulting in a probing depth of about 10 nm. The x-ray incidence angle was about 15°, and the photoelectron detection angle was 90°. The diameter of the beam spot was about 50 μm. The samples were covered with a thick layer of carbon paint after mounting onto the sample holders and then were fractured under ultrahigh vacuum of $10^{-6}$ Pa at room temperature in order to ensure that the photoemission signal from the sample is only obtained from a clean fractured surface that has not been previously exposed to air. The fractured sample surface was about 2 mm long along the beam direction and 100 μm wide. The measurements were performed at 80 and 150 K, corresponding to temperatures above and below its density wave transition at 140 K. The total energy resolution was about 300 meV. The binding energy of the HAXPES spectra was calibrated using the Fermi edge of Au.

## III. RESULTS AND DISCUSSION

Figure 2(a) shows a wide scan of $La_3Ni_2O_{7-\delta}$. As expected from the sample composition, the core level peaks of La, Ni, and O are observed, along with a C $1s$ signal originating from impurities at the grain boundaries in the polycrystal. Some signal from the carbon paint surrounding the sample cannot be ruled out due to the small size of the sample. Other than the carbon, no traces of core levels from other elements are detected in the scan.

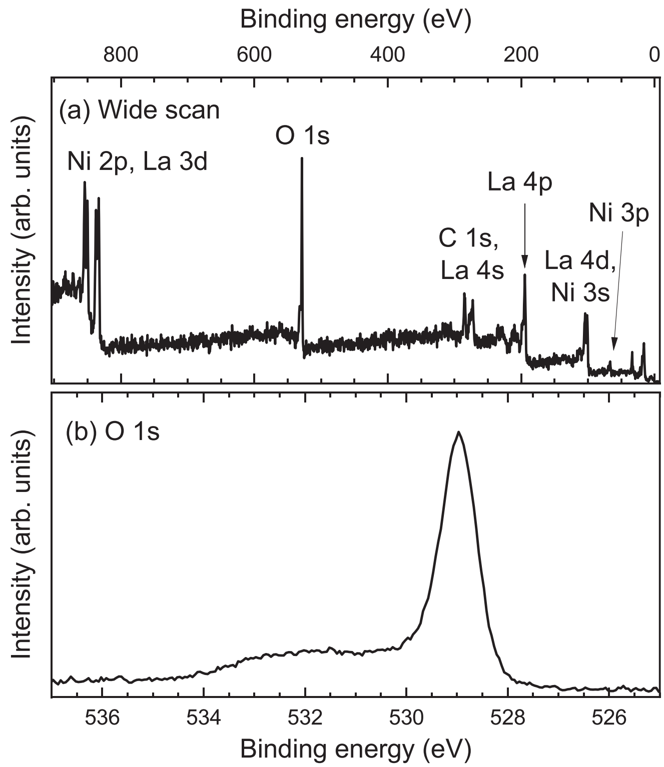


FIG. 2. (a) Wide scan and (b) O $1s$ core level spectra of the polycrystalline $La_3Ni_2O_{7-\delta}$.

The O $1s$ core level spectra of $La_3Ni_2O_{7-\delta}$, as shown in Fig. 2(b), consist of a main sharp peak, followed by a broad feature on the higher binding energy side originating from the impurities at grain boundaries. The sharp peak at 529 eV corresponds to the bulk $La_3Ni_2O_{7-\delta}$, and has a full width at half maximum (FWHM) of around 0.75 eV, close to that obtained from single-crystalline NiO under similar experimental conditions [32]. The bulk signal from $La_3Ni_2O_{7-\delta}$ dominates the O $1s$ spectra, indicating that our HAXPES spectra obtained from the present sample represent the bulk electronic structure.

Figure 3(a) shows the Ni $2p$ and La $3d$ core level spectra of $La_3Ni_2O_{7-\delta}$. The intense La $3d_{5/2}$ peak at around 835 eV displays a double-peak structure as often observed in lanthanum containing oxides such as the perovskites $LaMO_3$ [37]. The double-peak structure is derived from the core hole screening in the final states. The low- (high-) energy component corresponds to the $f^1$ ($f^0$) final state where the La $4f$ level stabilized by the La $3d$ core hole potential is occupied (unoccupied) by an electron. The same structure is then repeated at around 855 eV for La $3d_{3/2}$, which overlaps with the Ni $2p_{3/2}$ peak, expected to be at around the same binding energy. We note that this double-peak structure does match with the peaks that Liu *et al.* [27] attributed to $Ni^{2+}$ and $Ni^{3+}$, with the difference in experimental photon energies accounting for the different weight ratios between La $3d_{3/2}$ and Ni $2p_{3/2}$. We furthermore observe that in more isolated Ni $2p_{1/2}$, no such double-peak structure with 3–4 eV splitting and close to 1 : 1

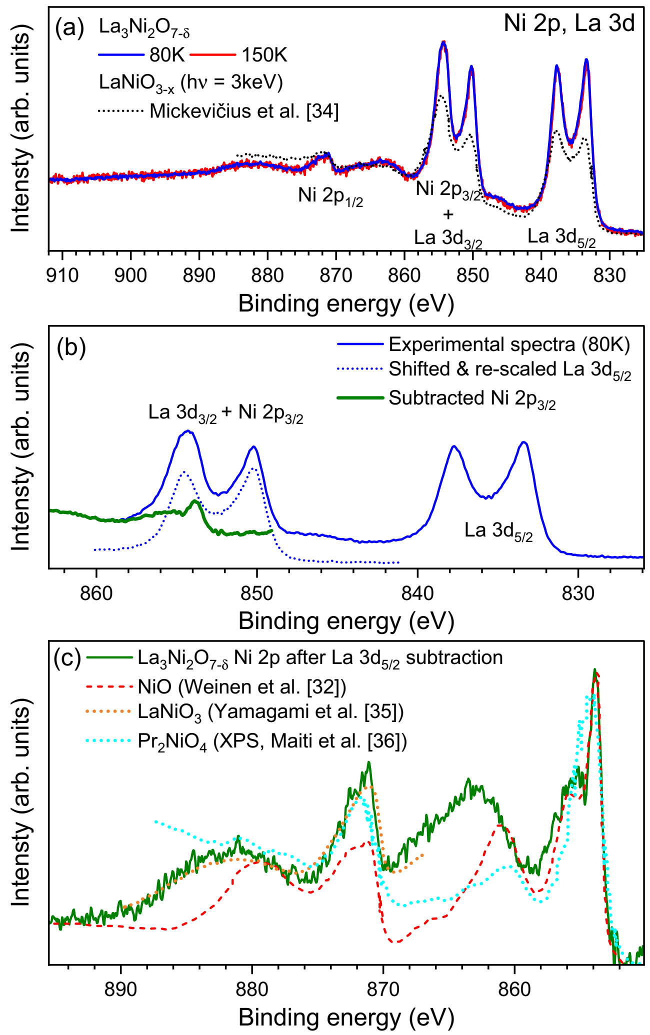


FIG. 3. (a) Ni $2p$ and La $3d$ core level spectra of polycrystalline $La_3Ni_2O_{7-\delta}$ measured at 80 K (blue line) and at 150 K (red line). [34] (b) Subtraction of La $3d_{3/2}$ by using the spectral shape of La $3d_{5/2}$ rescaled and shifted. (c) Ni $2p$ spectra after La $3d_{3/2}$ peak subtraction, together with the spectrum of NiO from Ref. [32], the Ni $2p_{1/2}$ spectrum of $LaNiO_3$ from Ref. [35], and the $Pr_2NiO_4$ x-ray photoemission spectroscopy (XPS) spectrum from Ref. [36].

ratio is observed, further evidencing that the splitting is on the La $3d$ core level and not on Ni $2p$.

In order to obtain more information despite this overlap, we can perform a subtraction of La $3d_{3/2}$ by assuming that the core level line shape is the same as that of La $3d_{5/2}$ [34]. For the subtraction, we shift La $3d_{5/2}$ to match the energy of the La $3d_{3/2}$ peak, and rescale it to account for the different number of electrons and photoionization cross section [blue dotted line in Fig. 3(b)]. The ratio of 1 : 1.34 obtained from the atomic values of the fully filled La $3d_{5/2}$ and La $3d_{3/2}$ photoionization cross section [38] was used as a starting point, and then fine tuned to fully cancel out the $f^1$ peak on La $3d_{3/2}$, between 849 and 851 eV.

The result of the subtraction, shown in Fig. 3(c), displays a two-peak structure [39], very similar in both shape and energy position to that of NiO [32], shown with the dashed red line. The main peak is accompanied by the broad charge-transfer

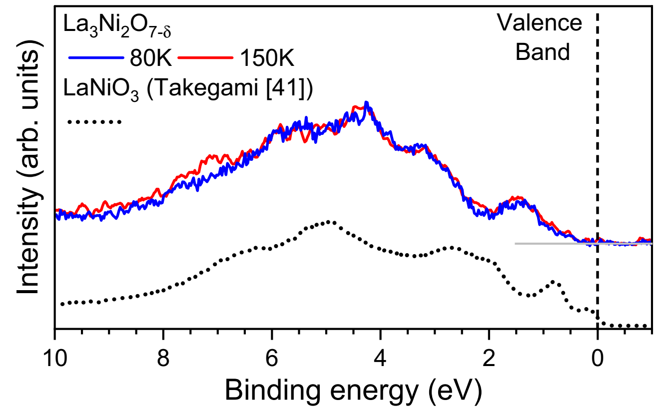


FIG. 4. HAXPES valence band spectra of polycrystalline $La_3Ni_2O_{7-\delta}$ measured at 80 K (blue line) and at 150 K (red line), together with that of $LaNiO_3$ (dotted line) from Ref. [41].

satellite on the higher binding energy side, matches closely to that of $LaNiO_3$ rather than to that of NiO. The more isolated Ni $2p_{1/2}$ peak at around 872 eV also displays a strong resemblance both to that of the formally $d^8$ NiO, as well as to that of $LaNiO_3$, with a ground state dominated by $d^8\underline{L}$. Here too we observe that the satellite structures display a strong similarity to that of $LaNiO_3$ rather than that of NiO.

In $La_3Ni_2O_{7-\delta}$, the nominal valence of Ni is +2.5 (+2.43 for $\delta \approx 0.07$). The striking similarities of the Ni $2p$ main peak to both NiO with a Ni valence of +2 and the $d^8\underline{L}$ $LaNiO_3$, rule out the coexistence of the Ni 2+ ($d^8$) and the actual Ni 3+ ($d^7$) states in $La_3Ni_2O_{7-\delta}$, and instead point towards the scenario where the electronic configuration of Ni is dominated by the $d^8\underline{L}$-$d^8$ mixture, with a Ni $3d$ to O $2p$ charge-transfer energy that is almost zero (or even negative).

Meanwhile, the satellite structure of $La_3Ni_2O_{7-\delta}$ is very different from those of NiO and $R_2NiO_4$ [32,36] with a positive charge-transfer energy of about 4 eV, both in terms of energy position as well as in weight. The broad charge-transfer satellite with the substantial energy splitting from the main peak is instead very similar to that of $LaNiO_3$ [34,35], with a very small or even negative charge-transfer energy as commonly found in many nominally Ni 3+ systems [28–31,40], further reinforcing the $d^8\underline{L}$-$d^8$ mixture scenario for $La_3Ni_2O_{7-\delta}$.

Figure 4 shows the valence band spectra of $La_3Ni_2O_{7-\delta}$. Similar to the spectra of $LaNiO_3$ (dotted line) as well as other rare-earth nickelates, it displays a broad deeper band from around 2 to 7 eV, and distinct features closer to the Fermi level mainly from the Ni $3d$ contributions. At high photon energies, the spectral weight of the deeper feature consists mostly of small La $5p$ contributions in the valence region from its hybridization with O and Ni valence states [35,42], which gets strongly enhanced and dominates the valence band spectra due to its very large photoionization cross sections.

Compared to $LaNiO_3$, we observe that the $La_3Ni_2O_{7-\delta}$ valence band features are all in general around 0.5 eV deeper, which is consistent with an electron doping of 0.5 electrons per Ni in going from $LaNiO_3$ to $La_3Ni_2O_7$. Furthermore, the features near the Fermi level appear to be broader, likely due to the density wave or its fluctuation by the electron doping to

$Ni^{3+}$ or the hole doping to $Ni^{2+}$. The Ni $3d$ $e_g$-O $2p$ band crossing the Fermi level is half filled in $LaNiO_3$ while it should be three quarters filled in $La_3Ni_2O_7$. We also note that $La_3Ni_2O_{7-\delta}$ shows a pseudogap behavior, with the spectral weight at the Fermi level being close to zero at both 80 and 150 K. The suppression of the spectral weight at the Fermi level is consistent with the barely metallic behavior under the ambient pressure which would be associated with the density wave and/or its fluctuation which is suggested from the kink of the resistivity curve around 140 K [18].

The density wave transition temperature gradually decreases with pressure and the superconductivity appears above the pressure where the density wave is almost suppressed [18]. Since the $Ni^{2+}/Ni^{3+}$ charge disproportion is absent as seen in the present Ni $2p$ HAXPES, the density wave should be associated with itinerant electrons constructed from Ni $3d$ $e_g$ and O $2p$ orbitals. If the density wave is driven by the conventional Peierls transition due to the electron lattice interaction, the Peierls gap is expected to close above the transition temperature. Since the spectral weight at the Fermi level is suppressed even above the transition temperature, the density wave transition at 140 K would be driven by an electron-electron interaction (or excitonic interaction) between Ni $3d$ electrons and/or O $2p$ holes. Then the pseudogap can remain even above the transition temperature due to their fluctuations. Such fluctuations can remain and induce the superconductivity under pressure while its long-range order is suppressed.

As suggested from the $f^1$ peaks in the La $3d$ spectra, the La $4f$ and $5d$ levels are not very far from the Fermi level. The La $5d$ level may be lowered by pressure and trigger the superconductivity. This situation with the La $5d$ Fermi surface resembles the situation of $NdNiO_2$ where the Ni $3d$ and Nd $5d$ Fermi surfaces coexist.

## IV. CONCLUSION

In conclusion, the HAXPES study on polycrystal $La_3Ni_2O_{7-\delta}$ ($\delta \approx 0.07$) has been used to study its electronic structure. The Ni $2p$ HAXPES spectra clearly show that the expected $Ni^{2+}/Ni^{3+}$ charge disproportionation is absent. The main peak and the charge-transfer satellite of Ni $2p$ HAXPES of $La_3Ni_2O_{7-\delta}$ point towards a $d^8\underline{L}$-$d^8$ ground state, indicating that oxygen $2p$ holes are heavily involved in the electronic states near the Fermi level. The spectral weight suppression at the Fermi level indicates that the carriers of O $2p$ character heavily mixed with Ni $3d$ are affected by electronic correlation which would be associated with the density wave transition and the superconductivity in the present system.

## ACKNOWLEDGMENTS

D.T. acknowledges the support by the Deutsche Forschungsgemeinschaft (DFG, German Research Foundation) under the Walter Benjamin Programme, Projektnummer 521584902. J.-G.C. is thankful for the support from the National Natural Science Foundation of China (12025408, 11921004), and the National Key R&D Program of China (2021YFA1400200). We acknowledge the support for the measurements from the Max Planck-POSTECH-Hsinchu Center for Complex Phase Materials.

[1] J. B. Goodenough, *Magnetism and the Chemical Bond* (Interscience, New York, 1963).

[2] M. Imada, A. Fujimori, and Y. Tokura, Metal-insulator transitions, Rev. Mod. Phys. **70**, 1039 (1998).

[3] D. I. Khomskii, *Transition Metal Compounds* (Cambridge University Press, Cambridge, UK 2014).

[4] J. B. Torrance, P. Lacorre, A. I. Nazzal, E. J. Ansaldo, and Ch. Niedermayer, Systematic study of insulator-metal transitions in perovskites $R$NiO$_3$ ($R$ = Pr,Nd,Sm,Eu) due to closing of charge-transfer gap, Phys. Rev. B **45**, 8209 (1992).

[5] M. T. Fernández-Díaz, J. A. Alonso, M. J. Martínez-Lope, M. T. Casais, J. L. García-Muñoz, and M. A. G. Aranda, Charge disproportionation in $R$NiO$_3$ perovskites, Phys. B: Condens. Matter **276-278**, 218 (2000).

[6] M. Azuma, W.-T. Chen, H. Seki, M. Czapski, S. Olga, K. Oka, M. Mizumaki, T. Watanuki, N. Ishimatsu, N. Kawamura, S. Ishiwata, M. G. Tucker, Y. Shimakawa, and J. P. Attfield, Colossal negative thermal expansion in $BiNiO_3$ induced by intermetallic charge transfer, Nat. Commun. **2**, 347 (2011).

[7] D. Li, K. Lee, B. Y. Wang, M. Osada, S. Crossley, H. R. Lee, Y. Cui, Y. Hikita, and H. Y. Hwang, Superconductivity in an infinite-layer nickelate, Nature (London) **572**, 624 (2019).

[8] G. A. Pan, D. Ferenc Segedin, H. LaBollita, Q. Song, E. M. Nica, B. H. Goodge, A. T. Pierce, S. Doyle, S. Novakov, D. Córdova Carrizales, A. T. N'Diaye, P. Shafer, H. Paik, J. T. Heron, J. A. Mason, A. Yacoby, L. F. Kourkoutis, O. Erten, C. M. Brooks, A. S. Botana *et al.*, Superconductivity in a quintuple-layer square-planar nickelate, Nat. Mater. **21**, 160 (2022).

[9] N. N. Wang, M. W. Yang, Z. Yang, K. Y. Chen, H. Zhang, Q. H. Zhang, Z. H. Zhu, Y. Uwatoko, L. Gu, X. L. Dong, J. P. Sun, K. J. Jin, and J.-G. Cheng, Pressure-induced monotonic enhancement of $T_c$ to over 30 K in superconducting $Pr_{0.82}Sr_{0.18}NiO_2$ thin films, Nat. Commun. **13**, 4367 (2022).

[10] J. Zaanen, G. A. Sawatzky, and J. W. Allen, Band gaps and electronic structure of transition-metal compounds, Phys. Rev. Lett. **55**, 418 (1985).

[11] T. Mizokawa and A. Fujimori, Electronic structure and orbital ordering in perovskite-type $3d$ transition-metal oxides studied by Hartree-Fock band-structure calculations, Phys. Rev. B **54**, 5368 (1996).

[12] T. Mizokawa, D. I. Khomskii, and G. A. Sawatzky, Spin and charge ordering in self-doped Mott insulators, Phys. Rev. B **61**, 11263 (2000).

[13] S. Johnston, A. Mukherjee, I. Elfimov, M. Berciu, and G. A. Sawatzky, Charge disproportionation without charge transfer in the rare-earth-element nickelates as a possible mechanism for the metal-insulator transition, Phys. Rev. Lett. **112**, 106404 (2014).

[14] R. J. Green, M. W. Haverkort, and G. A. Sawatzky, Bond disproportionation and dynamical charge fluctuations in the perovskite rare-earth nickelates, Phys. Rev. B **94**, 195127 (2016).

[15] A. Paul, A. Mukherjee, I. Dasgupta, A. Paramekanti, and T. Saha-Dasgupta, Hybridization-switching induced Mott transition in $ABO_3$ perovskites, Phys. Rev. Lett. **122**, 016404 (2019).

[16] H. Sun, M. Huo, X. Hu, J. Li, Z. Liu, Y. Han, L. Tang, Z. Mao, P. Yang, B. Wang, J. Cheng, D.-X. Yao, G.-M. Zhang, and M. Wang, Signatures of superconductivity near 80 K in a nickelate under high pressure, Nature (London) **621**, 493 (2023).

[17] J. Hou, P. T. Yang, Z. Y. Liu, J. Y. Li, P. F. Shan, L. Ma, G. Wang, N. N. Wang, H. Z. Guo, J. P. Sun, Y. Uwatoko, M. Wang, G. M. Zhang, B. S. Wang, and J. G. Cheng, Emergence of high-temperature superconducting phase in the pressurized $La_3Ni_2O_7$ crystals, Chin. Phys. Lett. **40**, 117302 (2023).

[18] G. Wang, N. N. Wang, X. L. Shen, J. Hou, L. Ma, L. F. Shi, Z. A. Ren, Y. D. Gu, H. M. Ma, P. T. Yang, Z. Y. Liu, H. Z. Guo, J. P. Sun, G. M. Zhang, S. Calder, J. -Q. Yan, B. S. Wang, Y. Uwatoko, and J.-G. Cheng, Pressure-induced superconductivity in polycrystalline $La_3Ni_2O_7$, arXiv:2309.17378 [Phys. Rev. X (to be published)].

[19] Z. Luo, X. Hu, M. Wang, W. Wú, and D.-X. Yao, Bilayer two-orbital model of $La_3Ni_2O_7$ under pressure, Phys. Rev. Lett. **131**, 126001 (2023).

[20] Y. Zhang, L.-F. Lin, A. Moreo, and E. Dagotto, Electronic structure, orbital-selective behavior, and magnetic tendencies in the bilayer nickelate superconductor $La_3Ni_2O_7$ under pressure, Phys. Rev. B **108**, L180510 (2023).

[21] F. Lechermann, J. Gondolf, S. Bötzel, and I. M. Eremin, Electronic correlations and superconducting instability in $La_3Ni_2O_7$ under high pressure, Phys. Rev. B **108**, L201121 (2023).

[22] H. Sakakibara, N. Kitamine, M. Ochi, and K. Kuroki, Possible high $T_c$ superconductivity in $La_3Ni_2O_7$ under high pressure through manifestation of a nearly-half-filled bilayer Hubbard model, Phys. Rev. Lett. **132**, 106002 (2024).

[23] Y. Gu, C. Le, Z. Yang, X. Wu, and J. Hu, Effective model and pairing tendency in bilayer Ni-based superconductor $La_3Ni_2O_7$, arXiv:2306.07275.

[24] Y. Shen, M. Qin, and G.-M. Zhang, Effective bi-layer model Hamiltonian and density-matrix renormalization group study for the high-$T_c$ superconductivity in $La_3Ni_2O_7$ under high pressure, Chin. Phys. Lett. **40**, 127401 (2023).

[25] X.-Z. Qu, D.-W. Qu, J. Chen, C. Wu, F. Yang, W. Li, and G. Su, Bilayer $t$-$J$-$J_\perp$ model and magnetically mediated pairing in the pressurized nickelate $La_3Ni_2O_7$, Phys. Rev. Lett. **132**, 036502 (2024).

[26] Yi-feng Yang, G.-M. Zhang, and F.-C. Zhang, Inter-layer valence bonds and two-component theory for high-$T_c$ superconductivity of $La_3Ni_2O_7$ under pressure, Phys. Rev. B **108**, L201108 (2023).

[27] Z. Liu, H. Sun, M. Huo, X. Ma, Y. Ji, E. Yi, L. Li, H. Liu, J. Yu, Z. Zhang, Z. Chen, F. Liang, H. Dong, H. Guo, D. Zhong, B. Shen, S. Li, and M. Wang, Evidence for charge and spin density waves in single crystals of $La_3Ni_2O_7$ and $La_3Ni_2O_6$, Sci. China: Phys., Mech. Astron. **66**, 217411 (2023).

[28] H. Eisaki, S. Uchida, T. Mizokawa, H. Namatame, A. Fujimori, J. van Elp, P. Kuiper, G. A. Sawatzky, S. Hosoya, and H. Katayama-Yoshida, Electronic structure of $La_{2-x}Sr_xNiO_4$ studied by photoemission and inverse-photoemission spectroscopy, Phys. Rev. B **45**, 12513 (1992).

[29] J. van Elp, H. Eskes, P. Kuiper, and G. A. Sawatzky, Electronic structure of Li-doped NiO, Phys. Rev. B **45**, 1612 (1992).

[30] S. R. Barman, A. Chainani, and D. D. Sarma, Covalency-driven unusual metal-insulator transition in nickelates, Phys. Rev. B **49**, 8475 (1994).

[31] T. Mizokawa, A. Fujimori, T. Arima, Y. Tokura, N. Mōri, and J. Akimitsu, Electronic structure of $PrNiO_3$ studied by photoemission and x-ray-absorption spectroscopy: Band gap and orbital ordering, Phys. Rev. B **52**, 13865 (1995).

[32] J. Weinen, T. C. Koethe, C. F. Chang, S. Agrestini, D. Kasinathan, Y. F. Liao, H. Fujiwara, C. Schüßler-Langeheine, F. Strigari, T. Haupricht, G. Panaccione, F. Offi, G. Monaco, S. Huotari, K.-D. Tsuei, and L. H. Tjeng, Polarization dependent hard x-ray photoemission experiments for solids: Efficiency and limits for unraveling the orbital character of the valence band, J. Electron Spectrosc. Relat. Phenom. **198**, 6 (2015).

[33] K. Momma and F. Izumi, *VESTA3* for three-dimensional visualization of crystal, volumetric and morphology data, J. Appl. Crystallogr. **44**, 1272 (2011).

[34] S. Mickevičius, S. Grebinskij, V. Bondarenka, B. Vengalis, K. Łliužienė, B.A. Orlowski, V. Osinniy, and W. Drube, Investigation of epitaxial $LaNiO_{3-x}$ thin films by high-energy XPS, J. Alloys Compd. **423**, 107 (2006).

[35] K. Yamagami, K. Ikeda, A. Hariki, Y. Zhang, A. Yasui, Y. Takagi, Y. Hotta, T. Katase, T. Kamiya, and H. Wadati, Hard x-ray photoemission study on strain effect in $LaNiO_3$ thin films, Appl. Phys. Lett. **118**, 161601 (2021).

[36] K. Maiti, P. Mahadevan, and D. D. Sarma, Evolution of electronic structure with dimensionality in divalent nickelates, Phys. Rev. B **59**, 12457 (1999).

[37] D. J. Lam, B. W. Veal, and D. E. Ellis, Electronic structure of lanthanum perovskites with 3$d$ transition elements, Phys. Rev. B **22**, 5730 (1980).

[38] M. B. Trzhaskovskaya and V. G. Yarzhemsky, Dirac–Fock photoionization parameters for HAXPES applications, At. Data Nucl. Data Tables **119**, 99 (2018).

[39] A. Hariki, Y. Ichinozuka, and T. Uozumi, Dynamical mean-field approach to Ni 2$p$ x-ray photoemission spectra of NiO: A role of antiferromagnetic ordering, J. Phys. Soc. Jpn. **82**, 043710 (2013).

[40] V. Bisogni, S. Catalano, R. J. Green, M. Gibert, R. Scherwitzl, Y. Huang, V. N. Strocov, P. Zubko, S. Balandeh, J.-M. Triscone, G. Sawatzky, and T. Schmitt, Ground-state oxygen holes and the metal–insulator transition in the negative charge-transfer rare-earth nickelates, Nat. Commun. **7**, 13017 (2016).

[41] D. Takegami, HAXPES on transition metal oxides: New insights into an effective use of the photoionization cross-sections., Ph.D. thesis, Technische Universität Dresden, 2023.

[42] D. Takegami, L. Nicolaï, T. C. Koethe, D. Kasinathan, C. Y. Kuo, Y. F. Liao, K. D. Tsuei, G. Panaccione, F. Offi, G. Monaco, N. B. Brookes, J. Minár, and L. H. Tjeng, Valence band hard x-ray photoelectron spectroscopy on 3$d$ transition-metal oxides containing rare-earth elements, Phys. Rev. B **99**, 165101 (2019).